

# Anisotropic superconductivity in graphite intercalation compound $\text{YbC}_6$

N.F. Kawai\*, Hiroshi Fukuyama

*Department of Physics, Graduate School of Science, The University of Tokyo,  
7-3-1 Hongo, Bunkyo-ku, Tokyo 113-0033, Japan*

---

## Abstract

We report anisotropy of the upper critical field ( $B_{c2}$ ) of an intercalated graphite superconductor  $\text{YbC}_6$  ( $T_c = 6.5$  K) determined from angular dependent magnetoresistance measurements. Though the perpendicular coherence length is much longer than interlayer spacing, measured angular dependences of  $B_{c2}$  are well fitted by the Lawrence-Doniach model or the Tinkham model, which are known to be applicable to quasi two-dimensional materials or thin films, rather than the effective mass model. This observation is similar to the measurements for the other intercalated graphite superconductor,  $\text{CaC}_6$ , by Jolibong et al. (Phys. Rev. B 76 (2007) 052511). A possible explanation for the unexpected applicability of these models is that our  $\text{YbC}_6$  samples are synthesized as thin flakes in the host graphite.

*Key words:* Superconductivity, Graphite intercalation, Layered material  
*PACS:* 74.70.Ad, 74.25.Fy, 74.25.Op

---

Graphite intercalation compounds (GICs) have been intensively studied for many years. This is because the electronic and magnetic properties can be controlled to a large extent by changing intercalant species and their arrangements such as the stage number and the intralayer structure [1]. Superconductivity is one of the most interesting properties among them. The superconducting transition temperature ( $T_c$ ) of GICs had been long limited below 3 K under ambient pressure [1]. The intercalants here are usually alkali metals. Recently, it was discovered that  $\text{CaC}_6$  and  $\text{YbC}_6$  have much higher  $T_c$  of 11.5 and 6.5 K, respectively [2]. Measured properties of these new *high- $T_c$*  GICs are well described with the framework of BCS theory [3,4,5,6,7]. Although the phonon mechanism is supposed to be relevant for their Cooper pairing [8], detailed microscopic mechanisms for the attractive interactions have not been fully understood yet.

---

\* Corresponding author. Tel.: +81 3 5841 8364; fax: +81 3 5841 8364.  
*Email address:* kawai@kelvin.phys.s.u-tokyo.ac.jp (N.F. Kawai).

Since GICs are structurally anisotropic, the superconducting properties also show anisotropic features. For instance, the upper critical field ( $B_{c2}$ ) of  $\text{KHgC}_8$  shows angular dependences which are well fitted by the effective mass (EM) model [9]. On the other hand, the anisotropy of  $B_{c2}$  in  $\text{CaC}_6$  is accounted for by the Lawrence-Doniach (LD) model or the Tinkham model [10], though these models are applicable mainly to quasi two-dimensional (2D) materials or thin films. Here we report measurements of angular dependent magnetoresistance in  $\text{YbC}_6$ . The anisotropy of  $B_{c2}$  deduced from our data is well described by the LD model or the Tinkham model. We infer that this result comes from a flake-shaped distribution of  $\text{YbC}_6$  in the host graphite in our sample.

The  $\text{YbC}_6$  samples were synthesized from the host material, a highly oriented pyrolytic graphite (HOPG) [11], by the vapor transport method. A pellet of Yb and a piece of HOPG were vacuum-sealed in a glass ampule, and heat-treated at 400 °C for 2 days. After cooling down, the glass ampule was opened inside a glove box with  $\text{N}_2$  flow, because  $\text{YbC}_6$  is extremely reactive to air. In the case of samples for transport measurements, Au lead wires were attached on HOPG with Ag paste before the heating. The typical sample size is about  $5 \times 2 \times 0.3 \text{ mm}^3$ .

The synthesized samples were first analyzed by X-ray diffraction (XRD) with  $\text{CuK}\alpha$  radiation at room temperature. The sample surfaces for the XRD measurements were protected with adhesive tapes against reaction in air. Fig. 1 is a measured XRD spectrum for such a sample showing both  $\text{YbC}_6$  (00l) peaks and host graphite ones. The interlayer spacing ( $d'$ ) deduced from this spectrum is 0.456 nm which is almost the same as the value reported by Weller et al. [2].

DC magnetization measurements in magnetic fields ( $B$ ) parallel to the  $ab$ -plane of  $\text{YbC}_6$  were carried out with a SQUID magnetometer [12]. The inset of Fig. 2 shows temperature dependences of magnetization ( $M$ ) measured at  $B = 1 \text{ mT}$  by field cooling (FC, closed circles) and zero field cooling (ZFC, open circles). It shows  $T_c = 6.5 \text{ K}$ , and an estimated superconducting volume fraction is a few percent. Field dependences of  $M$  measured at various fixed temperatures are shown in Fig. 2. In this plot, linear background signals, which are at most  $6 \times 10^{-3} \text{ emu}$  at  $B = 1 \text{ T}$ , have already been subtracted from the raw data. The origin of this background signal is not known at present. At each temperature, the upper critical field in the parallel direction ( $B_{c2\parallel}$ ) is determined as a field where magnetization returns to zero as indicated by the arrows in the figure.

Resistance measurements across the  $ab$ -plane were carried out using the standard 4-probe method [13] down to  $T = 2 \text{ K}$ . A measurement current was fixed at 1 mA. Sample surfaces for the transport measurements were protected with epoxy resin against reaction in air. Fig. 3 shows the temperature dependence

of resistance ( $R$ ) in zero magnetic field. The  $T_c$  value ( $= 6.47$  K) here is defined as  $R(T_c) = \frac{1}{2} R(T = 6.6$  K) (see the inset of Fig. 3). This is consistent with the  $T_c$  value determined from the magnetization measurements. The transition width corresponding to a resistance change from  $0.1$  to  $0.9R(T = 6.6$  K) is  $0.1$  K. Note that  $R$  decreases to zero at  $T \leq 6.4$  K, implying that superconducting paths connect the two voltage leads in spite of the small volume fraction of  $\text{YbC}_6$  in the host.

Field dependences of resistance measured at various fixed temperatures are shown in Fig. 4. The field is applied parallel to the  $ab$ -plane. At each temperature, the resistance increases rather sharply above a certain field which corresponds to  $B_{c2\parallel}$  as will be discussed later. With further increasing field, it approaches gradually to a universal curve ( $R_n(B)$ ) in the normal state whose apparent field dependence is governed by the host material. Note that the magnetoresistance of graphite is very large [14].

$B_{c2\parallel}$  values determined in this way are plotted as a function of temperature by the closed circles in Fig. 5.  $B_{c2\parallel}$  varies linearly with  $T$  in the measured temperature range ( $2$  K  $\leq T \leq T_c$ ). There are in good agreement with those determined from the magnetization measurements shown by the crosses in the figure. This consistency suggests appropriateness of the two independent determinations of  $B_{c2\parallel}$ . The open circles are fields where  $R(B) = \frac{1}{2} R_n(B)$ . This is not an appropriate definition for  $B_{c2\parallel}$ , since they are substantially (by  $\sim 65$  %) larger than the  $B_{c2\parallel}$  values determined from the magnetization measurements.

Next, we show results of resistance measurements in magnetic fields of various directions in Fig. 6. We define  $\theta$  as an angle between the field direction and the  $c$ -axis of  $\text{YbC}_6$ . As  $\theta$  decreases from  $90^\circ$  to  $0^\circ$ , the field dependence of  $R_n(B)$  becomes steeper reflecting the anisotropic magnetoresistance of host graphite [14]. From these data, temperature dependences of  $B_{c2}$  in various field directions are obtained (Fig. 7). The  $T$ -linear dependence of  $B_{c2}$  holds for any  $\theta$ . Angular dependences of  $B_{c2}$  at various fixed temperatures are also obtained from the data in Fig. 6 and plotted in Fig. 8. At any temperature,  $B_{c2}$  is anisotropic and a cusp is observed around  $\theta = 90^\circ$ .

We now compare the measured properties of  $\text{YbC}_6$  with three different theoretical models for anisotropic superconductivity in layered materials or thin films. The first one is the EM model [15], which introduces the anisotropy of the effective mass into the GL equations. This model deals superconductors as anisotropic continua, and is relevant when the coherence length perpendicular to layers is much longer than the interlayer spacing. In this model, the angular

dependence of  $B_{c2}$  is given by

$$\left(\frac{B_{c2}(\theta) \sin \theta}{B_{c2\parallel}}\right)^2 + \left(\frac{B_{c2}(\theta) \cos \theta}{B_{c2\perp}}\right)^2 = 1, \quad (1)$$

where  $B_{c2\perp}$  is the upper critical field in perpendicular direction. Also, relations between  $B_{c2}$  and the coherence length ( $\xi$ ) are given by

$$B_{c2\perp}(T) = \frac{\Phi_0}{2\pi\xi_{\parallel}(T)^2} = \frac{\Phi_0}{2\pi\xi_{\parallel}(0)^2} \left(1 - \frac{T}{T_c}\right) \quad (T \approx T_c) \quad (2)$$

and

$$B_{c2\parallel}(T) = \frac{\Phi_0}{2\pi\xi_{\parallel}(T)\xi_{\perp}(T)} = \frac{\Phi_0}{2\pi\xi_{\parallel}(0)\xi_{\perp}(0)} \left(1 - \frac{T}{T_c}\right) \quad (T \approx T_c). \quad (3)$$

Here  $\Phi_0 = h/2e$  is the flux quantum, and  $\xi_{\perp}$  and  $\xi_{\parallel}$  are coherence lengths perpendicular and parallel to layers, respectively. From Eq. (2), Eq. (3) and the data in Fig. 7,  $\xi_{\perp}$  and  $\xi_{\parallel}$  are estimated as

$$\xi_{\perp}(0) = 17 \text{ nm}, \quad (4)$$

$$\xi_{\parallel}(0) = 37 \text{ nm}. \quad (5)$$

This  $\xi_{\perp}(0)$  value is much larger than the interlayer spacing  $d' = 0.456$  nm, which does not exclude the applicability of the EM model. However, as shown in Fig. 8, fitting of the angular dependences of  $B_{c2}$  to Eq. (1) is poor (dashed lines). Particularly, this model does not represent the cusps around  $\theta = 90^\circ$ .

There are two other models which may be applicable to our data. They are the LD model [16] and the Tinkham model [17]. The LD model describes anisotropic superconductors as stacked 2D superconducting layers connected by Josephson coupling. On the other hand, the Tinkham model is to describe superconducting thin films. In both models, the angular dependence of  $B_{c2}$  is given by

$$\left|\frac{B_{c2}(\theta) \sin \theta}{B_{c2\parallel}}\right| + \left(\frac{B_{c2}(\theta) \cos \theta}{B_{c2\perp}}\right)^2 = 1. \quad (6)$$

These two models provide much better fittings for the measured angular dependences in Fig. 8 (solid lines). This suggests the thin film nature of our sample. Since  $\xi_{\perp} \gg d'$ , it would be hard to apply the LD model to the present results. Instead,  $\text{YbC}_6$  might be synthesized as thin flakes in the host acting as independent superconducting thin films. This is conceivable for the following reason. The host HOPG contains high-density stacking faults, and its effective thickness is estimated to be around 40 layers ( $\sim 13$  nm) [18]. So, it is likely that the thickness of synthesized  $\text{YbC}_6$  is also restricted by this layer number.

With the Tinkham model, other measured properties of our sample can be explained. First, a possible thickness variation in the superconducting paths

would broaden the resistive transition in magnetic fields, since  $B_{c2}$  increases with decreasing thickness in thin film superconductors [19]. Next, the fact that the  $B_{c2}$  values measured in this work are larger than those by Weller et al. [2] for  $\theta = 90^\circ$  (see Fig. 7) may be also due to the thinner effective thickness of our sample. However, such a difference is not seen at  $T \geq 4$  K for  $\theta = 0^\circ$ , for which we don't have reasonable explanation at this moment.

There remain a few points which are not accounted for by the Tinkham model. For instance, the measured  $B_{c2}$  at  $\theta = 90^\circ$  shows  $T$ -linear dependence rather than  $\sqrt{T_c - T}$  dependence:

$$B_{c2}(T) = \sqrt{12} \frac{\Phi_0}{2\pi\xi d} \propto \sqrt{T_c - T} \quad (7)$$

predicted by this model. Here,  $d$  is film thickness. The same disagreement has been reported by Jobiliong et al. [10] even for a bulk GIC superconductor, i.e.  $\text{CaC}_6$  synthesized from HOPG by the direct reaction method. On the other hand, for  $\text{YbC}_6$ , the temperature dependence of  $B_{c2}$  at  $\theta = 90^\circ$  measured by Weller et al. [2] is not linear with  $T$  nor  $\sqrt{T_c - T}$ . In order to solve this puzzle, future synthesis of  $\text{YbC}_6$  from single crystal graphite in well-defined form such as bulk is highly desirable.

In conclusion, we synthesized  $\text{YbC}_6$ , a superconducting GIC with  $T_c = 6.5$  K, by the vapor transport method. The measured angular dependences of  $B_{c2}$  at various field directions are well fitted by the Lawrence-Doniach (LD) model or the Tinkham model. This indicates the thin film nature of sample, which might originate from the thin film nature of host HOPG with high-density stacking faults. This scenario including the currently unexplained temperature dependence of  $B_{c2}$  will be tested by synthesizing sample with better defined form in future.

## Acknowledgments

We would like to thank C. Winkelmann and H. Kambara for their contributions in the early stage of this work. We would also like to thank S. Uchida and J. Shimoyama for their helpful suggestions in the magnetization and XRD measurements, and N. Akuzawa, Y. Iye and T. Matsui for valuable discussions. This work was financially supported by Grant-in-Aid for Scientific Research on Priority Areas (No. 17071002) from MEXT, Japan.

## References

- [1] T. Enoki, M. Suzuki, M. Endo, Graphite Intercalation Compounds and Applications, Oxford University Press, NY, 2003.
- [2] T. E. Weller, M. Ellerby, S. S. Saxena, R. P. Smith, N. T. Skipper, Nature Phys. 1 (2005) 39.
- [3] G. Lamura, M. Aurino, G. Cifariello, E. Di Gennaro, A. Andreone, N. Emery, C. Hérold, J-F. Marêché, P. Lagrange, Phys. Rev. Lett. 96 (2006) 107008.
- [4] J.S. Kim, R.K. Kremer, L. Boeri, F.S. Razavi, Phys. Rev. Lett. 96 (2006) 217002.
- [5] N. Bergeal, V. Dubost, Y. Noat, W. Sacks, D. Roditchev, N. Emery, C. Hérold, J-F. Marêché, P. Lagrange, G. Loupiau, Phys. Rev. Lett. 97 (2006) 077003.
- [6] M. Sutherland, N. Doiron-Leyraud, L. Taillefer, T. Weller, M. Ellerby, S. . Saxena, Phys. Rev. Lett. 98 (2007) 067003.
- [7] A. Akrap, T. Weller, M. Ellerby, S.S. Saxena, G. Csanyi, L. Forro, Phys. Rev. B 76 (2007) 045426.
- [8] I.I. Mazin, L. Boeri, O.V. Dolgov, A.A. Golubov, G.B. Bachelet, M. Giantomassi, O.K. Andersen, Physica C 460-462 (2007) 116.
- [9] Y. Iye, S. Tanuma, Phys. Rev. B 25 (1982) 4583.
- [10] E. Jobiliong, H.D. Zhou, J.A. Janik, Y-J. Jo, L. Balicas, J.S. Brooks, C.R. Wiebe, Phys. Rev. B 76 (2007) 052511.
- [11] Panasonic Graphite (grade STM Flat), Matsushita Electric Industrial Co., Ltd.
- [12] MPMS Model 1822, Quantum Design.
- [13] PPMS Model 6000, Quantum Design.
- [14] Z.M. Wang, Q.Y. Xub, G. Ni, Y.W. Dua, Phys. Lett. A 314 (2003) 328.
- [15] R.C. Morris, V. Coleman and R. Bhandari, Phys. Rev. B 5 (1972) 895.
- [16] W.E. Lawrence, S. Doniach, in: E. Kanda (Ed.), Proceedings of the 12th International Conference Low Temperature Physics, Shokabo, Tokyo, 1970, p.361.
- [17] M. Tinkham, Phys. Rev. 129 (1963) 2413.
- [18] T. Matsui, H. Kambara, Y. Niimi, K. Tagami, M. Tsukada and Hiroshi Fukuyama, Phys. Rev Lett. 94 (2005) 226403.
- [19] M. Tinkham, Introduction to Superconductivity, 2nd ed., McGraw-Hill, NY, 1996.

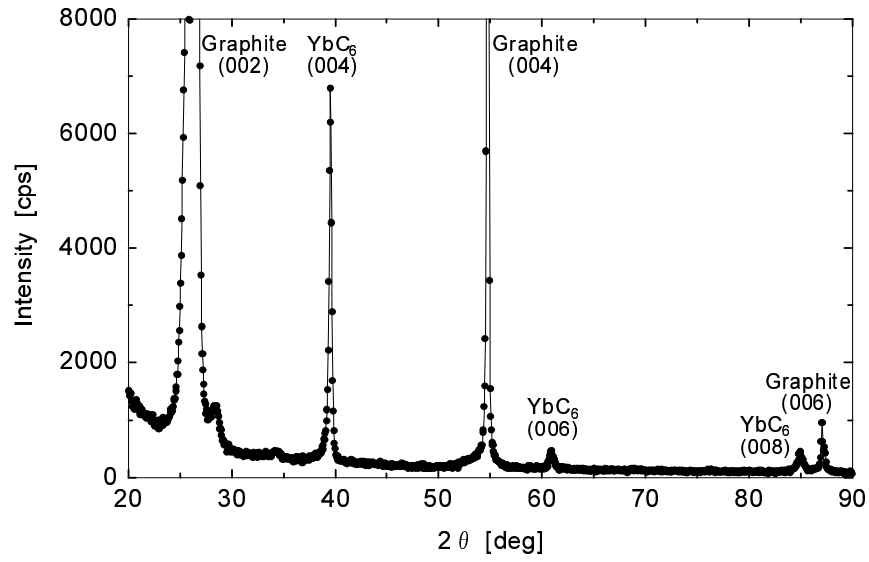


Fig. 1. The XRD spectrum of a synthesized YbC<sub>6</sub> sample measured with CuK $\alpha$  radiation at room temperature. Only (00l) peaks are observed because of the *c*-axis orientation of both host HOPG and YbC<sub>6</sub>.

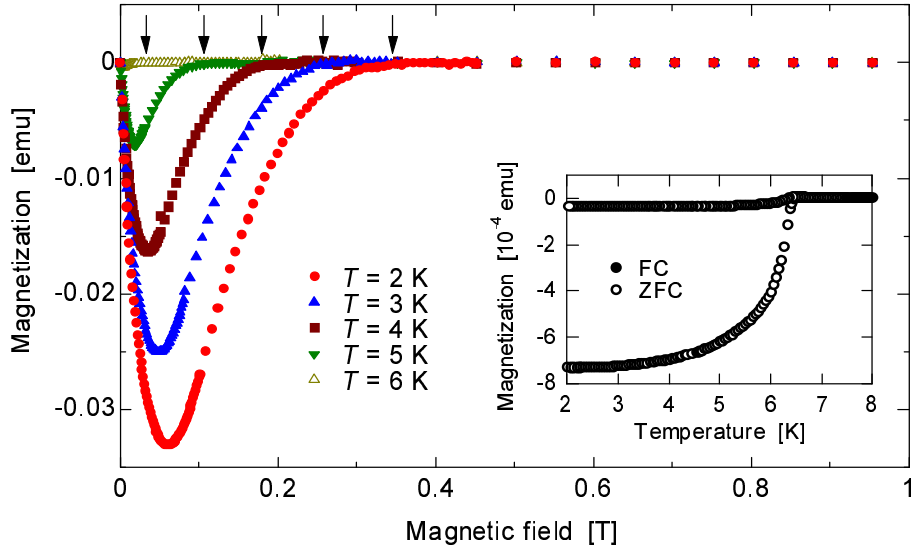


Fig. 2. The field dependence of magnetization in  $\text{YbC}_6$ . The field direction is parallel to the  $ab$ -plane. Linear background signals have already been subtracted from the raw data.  $B_{c2\parallel}$  values are indicated by the arrows. Inset: the temperature dependence of magnetization measured at  $B = 1 \text{ mT}$  ( $B \parallel ab$ -plane) with field cooling (FC) and zero field cooling (ZFC).



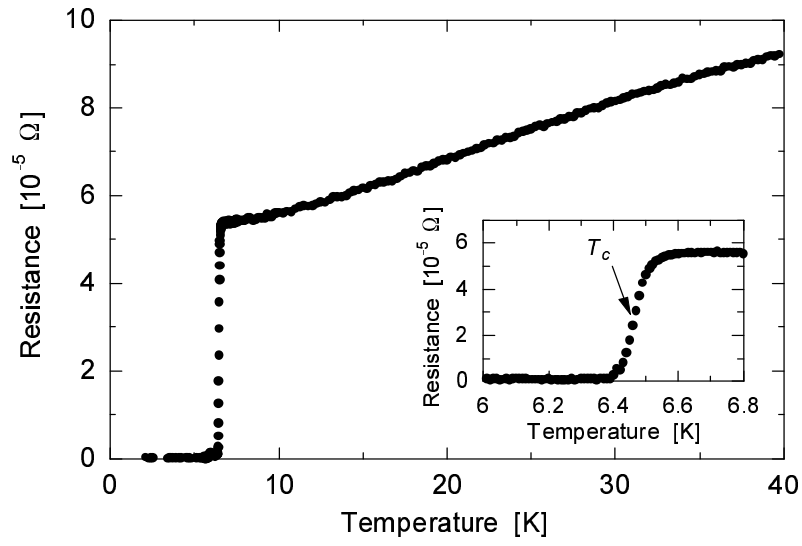


Fig. 3. The temperature dependence of resistance for  $\text{YbC}_6$  in zero magnetic field. Inset: the detailed resistance change near  $T_c$  ( $= 6.47$  K).

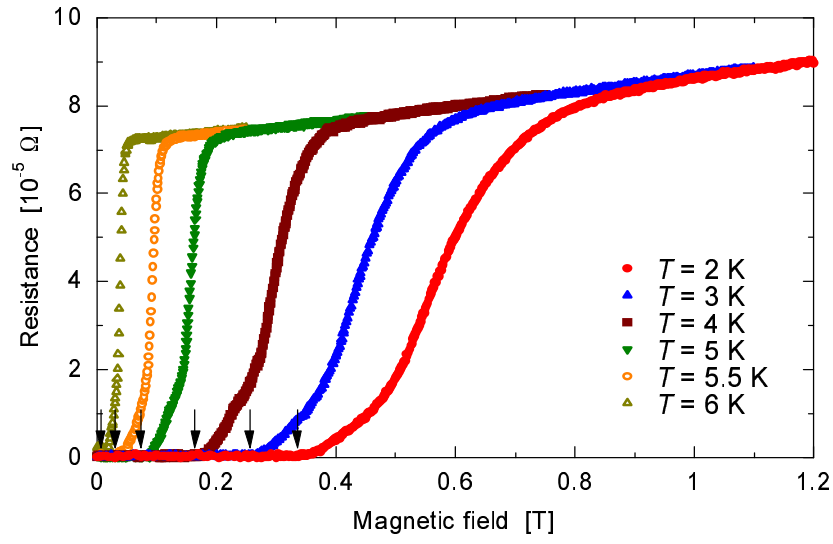


Fig. 4. The field dependence of resistance in YbC<sub>6</sub>. The field direction is parallel to the *ab*-plane. The arrows indicate  $B_{c2||}$  values where resistance becomes finite with increasing field.

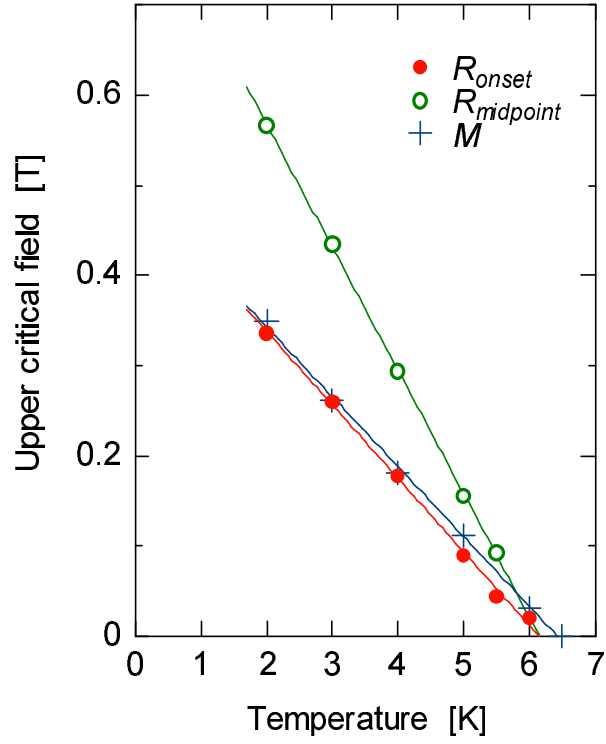


Fig. 5. The  $B_{c2\parallel}$  values of  $\text{YbC}_6$  determined from the transport measurements (circles) and the magnetization measurements (crosses). The open circles are fields defined as midpoints of the resistive transition, which are substantially larger than the  $B_{c2\parallel}$  values (see text).

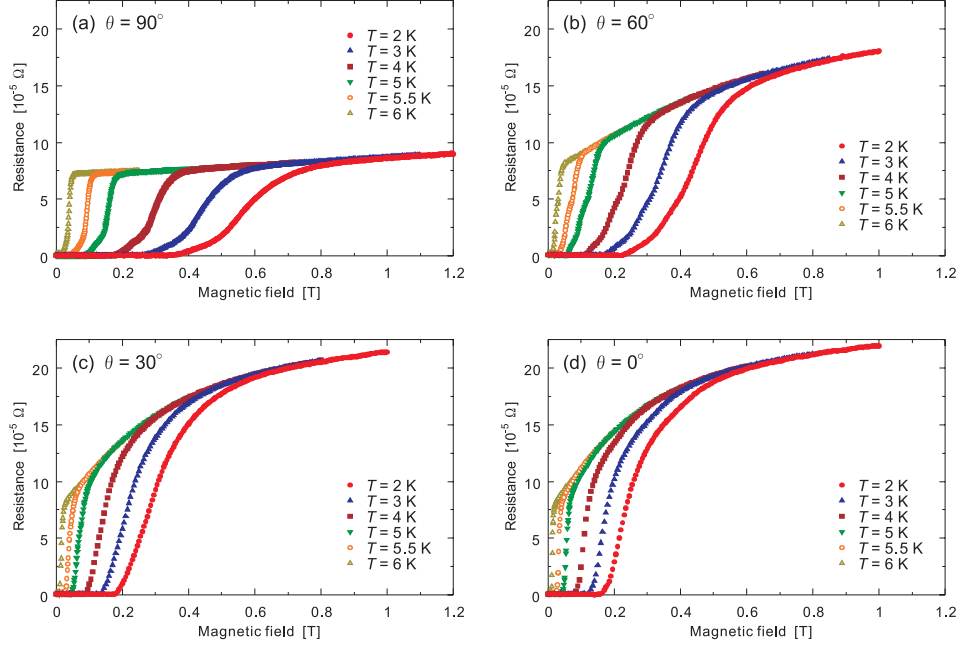


Fig. 6. The magnetic field dependences of resistance for YbC<sub>6</sub> in various field directions.  $\theta$  is defined as an angle between the magnetic field direction and the  $c$ -axis of YbC<sub>6</sub>. (a)  $\theta = 90^\circ$ ; (b)  $\theta = 60^\circ$ ; (c)  $\theta = 30^\circ$ ; (d)  $\theta = 0^\circ$ .

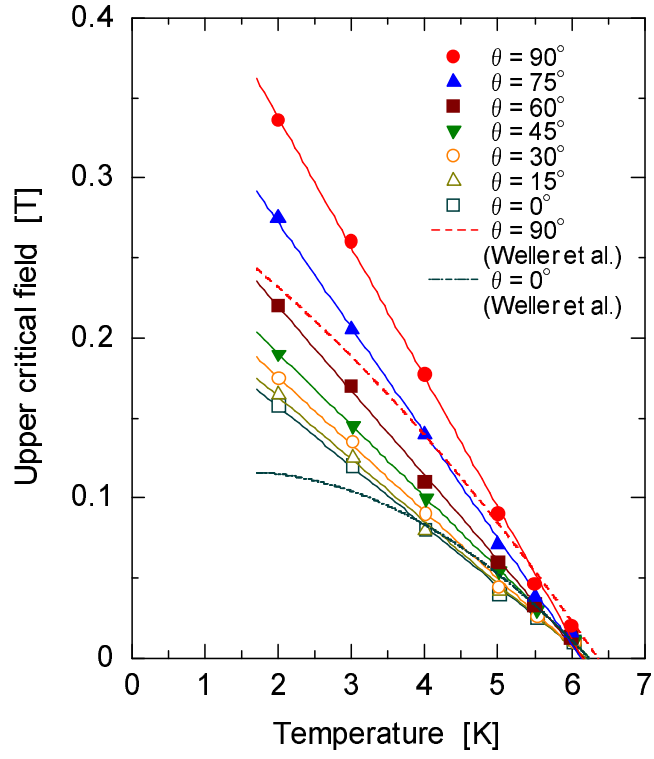


Fig. 7. The temperature dependences of  $B_{c2}$  for  $\text{YbC}_6$  in various field directions. The  $T$ -linear dependence of  $B_{c2}$  holds at any  $\theta$ . The dashed lines are from Weller et al. [2].

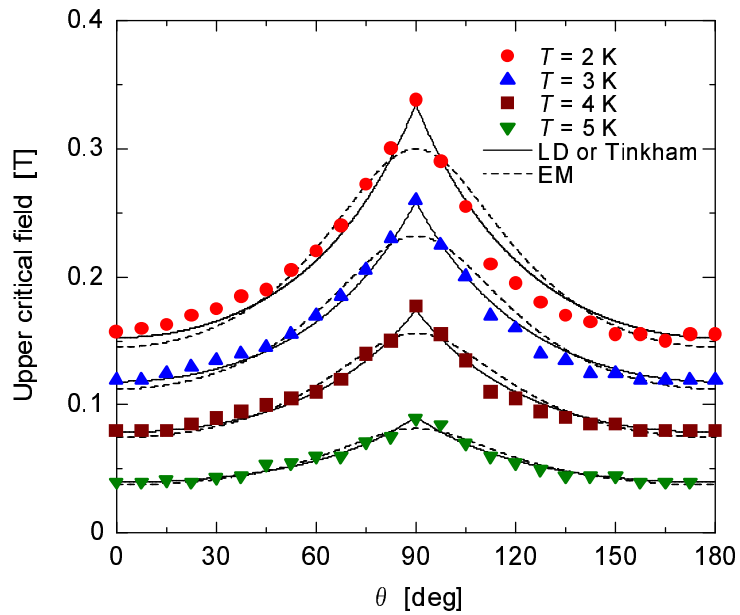


Fig. 8. The angular dependence of  $B_{c2}$  in YbC<sub>6</sub> at various fixed temperatures. Fittings with the EM model and the LD or Tinkham model are shown by the dashed lines and solid lines, respectively.